# Statistical Comparison of Trait-Dependent Biogeographical Models Indicates That Podocarpaceae Dispersal Is Influenced by Both Seed Cone Traits and Geographical Distance

Kristina V. Klaus[1,*] and Nicholas J. Matzke[2,3]

[1]*Department of Evolution and Biodiversity of Plants, Ruhr-Universität Bochum, Universitätsstraße 150, 44801 Bochum, Germany;* [2]*Moritz Laboratory, Division of Ecology and Evolution, Centre for Biodiversity Analysis, Research School of Biology, RN Robertson Bldg, Level 2, West Wing (W208), 46 Sullivans Creek Rd, Australian National University, Acton ACT 2601, Australia; and* [3]*School of Biological Sciences, 3A Symonds Street, The University of Auckland, Auckland 1010, New Zealand *Correspondence to be sent to: Department of Evolution and Biodiversity of Plants, Ruhr-Universität Bochum, Universitätsstraße 150, 44801 Bochum, Germany; E-mail: kristina.klaus@rub.de.*

*Abstract*.—The ability of lineages to disperse long distances over evolutionary timescales may be influenced by the gain or loss of traits adapted to enhance local, ecological dispersal. For example, some species in the southern conifer family Podocarpaceae have fleshy cones that encourage bird dispersal, but it is unknown how this trait has influenced the clade's historical biogeography, or its importance compared with other predictors of dispersal such as the geographic distance between regions. We answer these questions quantitatively by using a dated phylogeny of 197 species of southern conifers (Podocarpaceae and their sister family Araucariaceae) to statistically compare standard, trait-independent biogeography models with new BioGeoBEARS models where an evolving trait can influence dispersal probability, and trait history, biogeographical history, and model parameters are jointly inferred. We validate the method with simulation-inference experiments. Comparing all models, those that include trait-dependent dispersal accrue 87.5% of the corrected Akaike Information Criterion (AICc) model weight. Averaged across all models, lineages with nonfleshy cones had a dispersal probability multiplier of 0.49 compared with lineages with fleshy cones. Distance is included as a predictor of dispersal in all credible models (100% model weight). However, models with changing geography earned only 22.0% of the model weight, and models submerging New Caledonia/New Zealand earned only 0.01%. The importance of traits and distance suggests that long-distance dispersal over macroevolutionary timespans should not be thought of as a highly unpredictable chance event. Instead, long-distance dispersal can be modeled, allowing statistical model comparison to quantify support for different hypotheses. [BioGeoBEARS; avian endozoochory; historical biogeography; long-distance dispersal; New Caledonia; seed dispersal; trait-dependent dispersal models; New Zealand.]

Organismal traits can often be linked to the dispersal ability of a species (Vittoz and Engler 2007; Hintze et al. 2013; Van Den Elzen et al. 2016). For example, many plant diaspores (seeds or spores) exhibit adaptations for transport by wind (Hughes et al. 1994; Greene and Quesada 2005; Eriksson 2008) or animals (Sorensen 1986). Diaspores adapted to dispersal via ingestion by animals (endozoochory) offer edible rewards to attract particular seed dispersers. Birds, for instance, are typically attracted by reddish or blackish (but rarely by orange, yellow, green, or brown), fleshy diaspores (Willson et al. 1990).

Although the relevance of seed traits for the dispersal ability of a species is obvious, the importance of seed traits for what we term "macroevolutionary dispersal" is an open question. Macroevolutionary dispersal events are dispersal events so rare that their frequency is measurable only on macroevolutionary, that is phylogenetic, timescales spanning millions of years. Rare, long-distance dispersal events may have great evolutionary significance in explaining the geographical distribution of clades across multiple continents and remote islands. They may also explain why certain clades have diversified in some regions but not in others (e.g. de Queiroz 2014).

Seed dispersal mechanisms are primarily regarded as adaptations for "ecological dispersal," that is dispersal within the home range of a species. Studying the "dispersal kernels" of wind-dispersed species has shown that the vast majority of diaspores end up relatively close to the parent plant (Nathan 2006). Dispersal beyond the home range is likely to be disadvantageous for the vast majority of individuals, because most seeds would meet unsuitable conditions and fail to survive. Therefore, it is possible that inferred macroevolutionary dispersal events in the history of a particular clade are not correlated with adaptations for ecological dispersal. Rather, other traits could be the dominant predictor of macroevolutionary dispersal success, for example (i) the ability to survive floating in saltwater (Darwin 1859), (ii) the ability to self-fertilize after colonization (Baker 1955; Carlquist 1965), or (iii) being an "easy colonizer" thanks to a generalist lifestyle (Losos and Ricklefs 2009). For these reasons, the presumed correlation between a particular diaspore trait and macroevolutionary dispersal is not simply a given, but a hypothesis to be tested. Moreover, the scale of the effect of a diaspore trait on macroevolutionary dispersal ability should be measured, in order to distinguish between effects that are statistically detectable but of little importance, and effects that are important predictors of differences in macroevolutionary dispersal probability.

In this article, we present and test a new extension of the R package BioGeoBEARS in which macroevolutionary dispersal probability can be affected by a discrete trait that is itself evolving. We apply the model to southern-hemisphere conifers belonging to the families Podocarpaceae and Araucariaceae to test whether the

seed-bearing structures of these clades have influenced their macroevolutionary dispersal. Podocarpaceae consists of 18 genera which display marked differences in their reproductive structures (Schulz et al. 2014). The seed cones of several genera, like those of the species-rich genus *Podocarpus*, are composed of 1 or 2 seeds, each of which is covered by a fleshy or coriaceous layer known as the epimatium. Many Podocarpaceae have a soft and fleshy receptaculum, derived from modified cone bracts (Knopf 2011; Knopf et al. 2012), which can turn bright red or black at maturity. To ingest the fleshy receptacular tissue at the base of the stalk, birds must also swallow the seed together with the covering epimatium. Within this family, the morphology of the seed cones and the receptaculum (if present) is highly variable (Fig. 1). Based on the morphological characteristics of the seed cone, we predict endozoochory for 11 Podocarpaceae genera, including the genus *Podocarpus* which is only partly endozoochorously dispersed. The woody seed cones of the genus *Saxegothaea* lack a receptaculum (Fig. 1H) and are highly distinct from the fleshy cones of most members of the genus *Podocarpus* (Farjon 2010). Other genera (e.g. *Prumnopitys, Afrocarpus*, Fig. 1G,I) share the absence of a receptaculum, but possess a coriaceous (rather than fleshy), green or yellow seed cover (epimatium) (Farjon 2010; Knopf et al. 2012). In these cases, the diaspore is usually not swallowed whole by the disperser. Even if some birds chop and eat the coriaceous tissue, the seeds are less likely to be swallowed. Without the protection of the epimatium, seeds that are swallowed are less likely to survive the intestinal passage (Gautier-Hion et al. 1985). Hence, 7 genera of the Podocarpaceae (and *Podocarpus* species with nonfleshy seed cones) are usually not ornithochorous. All members of the sister family Araucariaceae have nonfleshy seed cones.

## GEOGRAPHICAL DISTANCES AND PALEOGEOGRAPHY IN BIOGEOGRAPHICAL MODELS

Apart from morphological traits, other factors may influence macroevolutionary dispersal probability. These include the distances between geographical areas, and changes in these distances due to plate tectonics (Leprieur et al. 2016). Biogeographical models which include geographical distance as a predictor of dispersal are well-developed (Webb and Ree 2012; Landis et al. 2013, 2018; Van Dam and Matzke 2016). Another factor which may influence the historical biogeography of a clade is the emergence and submergence of areas. The islands of New Caledonia and New Zealand are diversity hotspots for the Podocarpaceae and Araucariaceae. Both islands are home to many endemic species from a variety of genera. In New Caledonia, these include *Podocarpus, Retrophyllum, Dacrydium, Dacrycarpus, Acmopyle, Prumnopitys, Parasitaxus, Araucaria*, and *Agathis*. In New Zealand, the genera with high levels of endemism are *Podocarpus, Dacrydium, Dacrycarpus, Phyllocladus, Halocarpus, Lepidothamnus, Prumnopitys, Manoao*, and

*Agathis*. There is a long-running debate about whether these islands should be regarded as ancient Gondwanan refugia (e.g. Lowry 1998; Murienne et al. 2005), or as "Darwinian islands" which re-emerged after a period of total submergence (e.g. Grandcolas et al. 2008; Swenson et al. 2014).

## HISTORICAL BIOGEOGRAPHY AND SEED CONE EVOLUTION IN PODOCARPACEAE

Previous studies either used the fossil record of the Podocarpaceae alone to interpret the group's historical biogeography (e.g. Hill 1995; Brodribb and Hill 1999) or they combined phylogenies with data from the fossil record (e.g. Wagstaff 2004 [*Phyllocladus*], Leslie et al. 2012 [conifers]). Quiroga et al. (2016) used a single dispersal-extinction-cladogenesis model (DEC; Ree and Smith 2008) to estimate ancestral ranges and dispersal pathways for 49 *Podocarpus* species. Here, we hypothesize that fleshy cones, geographic distance, and paleogeography have influenced the macroevolutionary dispersal rate in Araucariaceae and Podocarpaceae. To test this, we construct a total of 48 models that include or exclude an effect of the fleshy/nonfleshy trait on macroevolutionary dispersal probability, and combine the trait-dependent dispersal model variant with distance-dependence and time-stratification to test whether the inclusion of changing distances and areas over geological time changes the inference of a trait-dependence effect.

## MATERIALS AND METHODS

### Phylogenetic Reconstruction and Molecular Dating

Sequences were downloaded from GenBank (Supplementary Table S1 available on Dryad at https://doi.org/10.5061/dryad.d117b3k). Six loci were used (Knopf et al. 2012; Little et al. 2013): *matK*, NEEDLY intron 2, *PHYP*, *rbc*L, the *trnL*-intron, and the *trnL-trnF* intergenic spacer region. Each locus was aligned separately in GENEIOUS 7.1.9 (Kearse et al. 2012). Each alignment was manually curated to remove any columns with ambiguous alignment or representation in only a few taxa, taking care to always keep protein-coding DNA in-frame (removing only 3 columns, representing a codon, at a time). The resulting alignment consisted of 197 taxa with a total length of 5337 bp. The entire sister family Araucariaceae was included as outgroup to prevent potential biases that could occur in dating analyses if just one species of a diverse sister group is used as outgroup. Concatenation was carried out with Sequence Matrix 1.7.8 (Vaidya et al. 2011). The dating analysis was performed using BEAST 2.4.3 (Bouckaert et al. 2014). PartitionFinder 2.1.1 (Lanfear et al. 2016) was used to find an optimal partitioning scheme; we used BIC in order to favor partitioning schemes that are slightly less complex and thus more likely to have sufficient data to ensure good mixing in
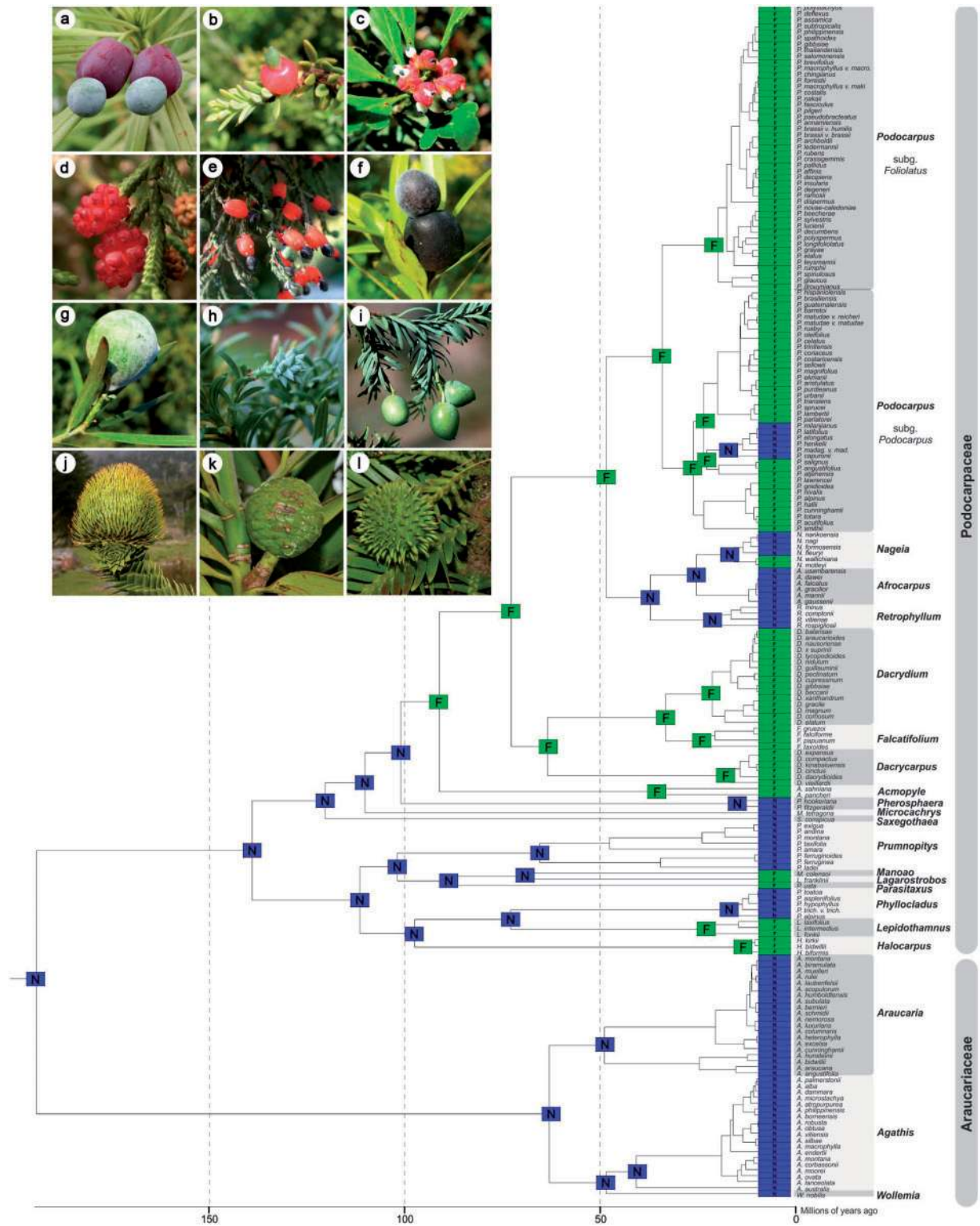
FIGURE 1.    Seed cones of the Podocarpaceae and Araucariaceae. a) *Podocarpus macrophyllus*, b) *Podocarpus nivalis*, c) *Phyllocladus asplenifolius*, d) *Microcachrys tetragona*, e) *Dacrycarpus dacrydioides*, f) *Podocarpus elatus*, g) *Afrocarpus falcatus*, h) *Saxegothaea conspicua*, i) *Prumnopitys amara*, j) *Araucaria araucana*, k) *Agathis robusta*, and l) *Wollemia nobilis*. Depicted at each node: the most-probable ancestral state for the seed cone fleshiness trait in Podocarpaceae and Araucariaceae under the best-fitting model (DIVALIKE+$j$+$x$+$t_{12}$+$t_{21}$+$m_2$). F (light nodes) = fleshy seed cone structures; N (dark nodes) = nonfleshy seed cone structures.

the BEAST2 MCMC. A 6-partition scheme was selected, with separate GTR+G+ estimated base frequencies models for each partition, except for one where GTR was replaced with HKY. The inferred partitioning scheme was reasonable (e.g., first codon positions from one locus were often grouped with first codon positions from other loci; Supplementary Data available on Dryad). We applied the lognormal uncorrelated relaxed clock model and birth–death tree prior. Three date calibrations from Leslie et al. (2012) were used: The split of the Araucariaceae and the Podocarpaceae was calibrated based on the macrofossil of *Araucarites rudicula* which was assigned to the Araucariaceae. This association is supported by the presence of Araucariacites pollen grains. The split was fixed at 176–230 Ma (95% confidence interval) with a normal prior distribution. The second calibration point was based on the fossil *Dacrycarpus puertae*, representing the split of *Dacrycarpus* and *Dacrydium+Falcatifolium*. This fossil was radiometrically dated to the Early Eocene (51.9 Ma). The split was fixed at 51.9–71.9 Ma (95% confidence interval) with a lognormal prior distribution. The split of *Phyllocladus* and *Halocarpus* was used as third calibration point, based on a number of *Phyllocladus* fossils which are described from the mid-Late Eocene (~37 Ma), as well as from the Early Eocene (48–55 Ma) of Tasmania (Brodribb and Hill 1999; Leslie et al. 2012). This split was fixed at 48–68 Ma (95% confidence interval) with a lognormal prior distribution. The MCMC analysis was run using a random starting tree and 100 million generations, sampling every 5000th generation. We used Tracer to confirm that all parameters had estimated sample sizes (ESS) >200. We discarded the first 2500 trees (25%) from each run as burn-in, and used the rest to generated the maximum clade credibility tree with TreeAnnotator.

### Classification of Seed Cone Traits

We classified the tip species into 2 categories, seed cone type fleshy (F) and nonfleshy (N), depending on their seed cone characteristic. Seed cone type F was defined as: red or black soft and fleshy seed cover with an additional red or black soft and fleshy receptacle (seeds dispersed by avian endozoochory). Seed cone type N was defined as: woody seed cones or a yellow, orange, red, or greenish (coriaceous) seed cover, no receptacle (seeds less likely dispersed by avian endozoochory). A trait file was created for BioGeoBEARS which contained the trait information "seed cone type F" or "seed cone type N" for each taxon.

### Geographical Data and Areas

We divided the world's land masses into 9 areas, representing all distribution areas of the Podocarpaceae and Araucariaceae (Fig. 2). We performed a fine-scale partitioning of the diversity hotspot of Australasia, Malesia (according to the latest edition of the World Geographical Scheme for Recording Plant Distributions [WGSRPD]), Papuasia including the Solomon Islands (according to the WGSRPD), and the Pacific islands (Fig. 2D–I), whereas America, Africa, and Asia (mainland) were each treated as a single area (Fig. 2A–C). We measured distance matrices for 4 different points in time: 0, 50, 100, and 150 Ma. Great Circle distances were generated by obtaining latitude and longitude coordinates of the closest edges of every pair of areas for each of the 4 time periods using paleomaps from GPlates (Müller et al. 2016), specifically https://portal.gplates.org/service/d3_demo/ on orthographic projection. A custom script using the R package geosphere (Hijmans 2016) was used to calculate the Great Circle distance from the paleo-longitude/latitude data. Only relative distances are needed for measuring the relationship of distance and dispersal, and scaling can be an issue in parameter estimation, so we divided all of the distances by the minimum observed distance in order to produce relative distance matrices that were used in the analysis.

### Biogeographical Inference using Trait-dependent Dispersal Models

We developed a new model variant in BioGeoBEARS which allows an evolving discrete trait to affect dispersal ability, and which in turn allows dispersal history to affect inference of trait evolution. We tested for a correlation between seed cone fleshiness and dispersal probability in Podocarpaceae by comparing the fit of models with trait-dependent dispersal to models where dispersal is independent of the trait. Models are compared by their fit to the data, where "the data" consist of both the geographic range data and the trait states for each species. Fit is measured with corrected Akaike Information Criterion (AICc) using standard procedures of statistical model comparison (Burnham and Anderson 2002).

The logic of trait-dependent dispersal models is well-explained by Sukumaran and Knowles (2018; see also Matos-Maraví et al. 2019; Lu et al. 2019). Such a model adds three additional free parameters to a standard BioGeoBEARS model. First, the parameters $t_{12}$ and $t_{21}$ describe the rate of transition of the morphological character from state 1 to state 2 (from F to N, that is, the rate of loss of the fleshy fruit state) and state 2 to state 1 (from N to F). This transition matrix is identical to the 2-rate model for a standard character available in the R package ape (Paradis et al. 2004), or the M*k*A model discussed by Pyron (2017). For comparison, a 1-rate model (the M*k* model of Lewis 2001) was also run on the trait data. The third parameter, $m_2$, is a multiplier on the base anagenetic dispersal rate $d$ (the rate of range expansion) when a lineage is in state 2. Parameter $m_1$ is also present in the model, representing a rate multiplier when the lineage is in state 1. However, in this analysis $m_1$ was fixed to 1, because $m_1$ and $m_2$ are not simultaneously identifiable along with the base
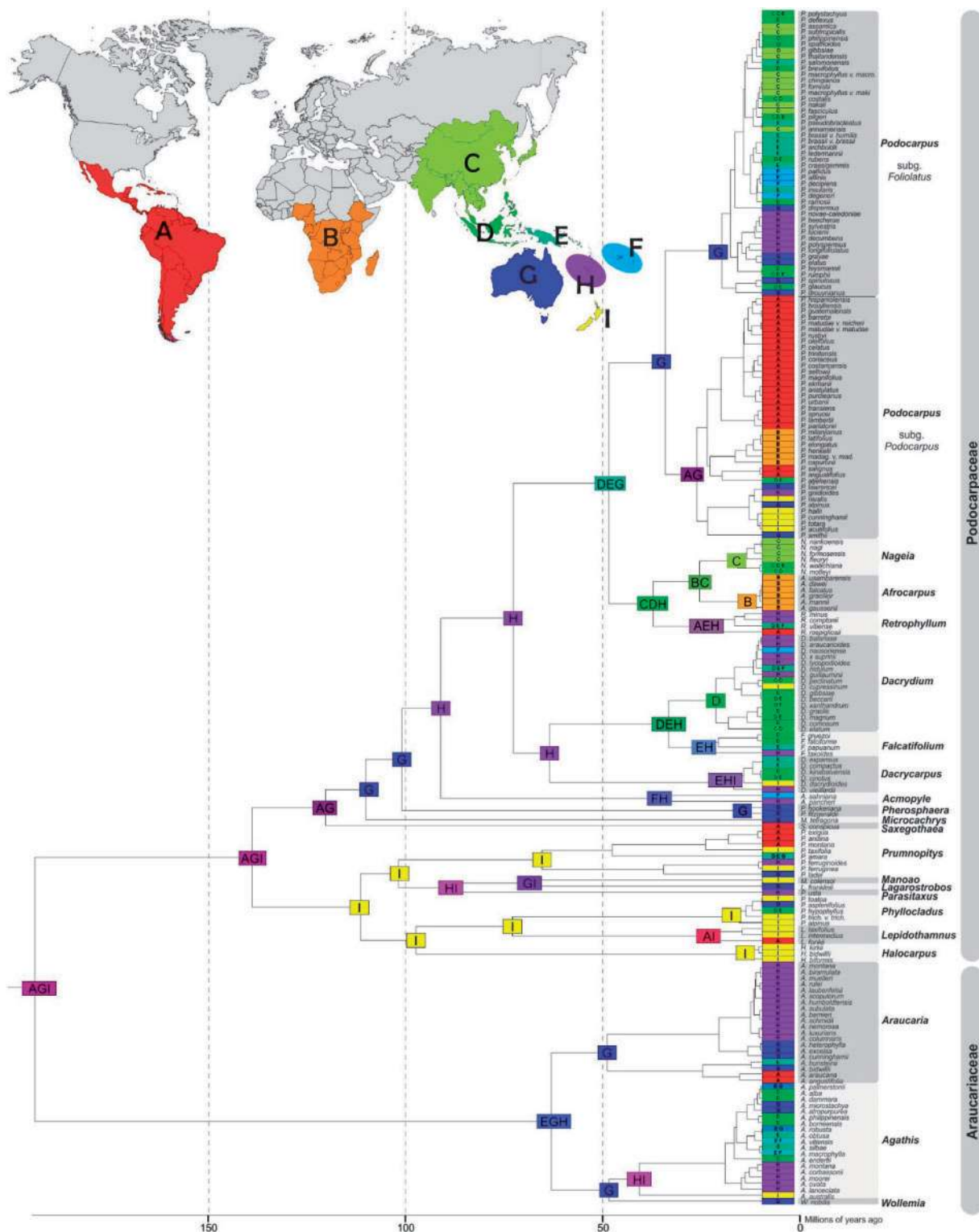
FIGURE 2. World distribution map and trait-dependent historical biogeography of the Podocarpaceae and Araucariaceae under the best-fitting model (DIVALIKE+$j$+$x$+$t_{12}$+$t_{21}$+$m_2$). A) Central and South America including the Caribbean, B) Africa and Madagascar, C) Asia (mainland), D) Malesia, E) Papuasia including the Solomon Islands, and Vanuatu, F) Fiji and Tonga, G) Australia and Tasmania, H) New Caledonia, and I) New Zealand.

dispersal parameters. For +$j$ model variants, the same multiplier is applied to $j$, the relative weight of founder-event jump dispersal during cladogenesis. We note that

it has recently been claimed that "DEC and DEC+J cannot be compared using standard statistical methods" (Ree and Sanmartín 2018). However, this argument

can be disproved on several fundamental grounds. For example, the identifiability of the $d$ and $j$ parameters was proven with simulation-inference experiments in Matzke (2014), whereas Ree and Sanmartín omitted simulation and instead argue from 2 small, human-constructed datasets (trees with 2 or 4 tips) – which we consider an insufficient basis on which to judge Maximum Likelihood inference of models with 2 or 3 free parameters. We briefly review these issues in Supplementary Material available on Dryad. A more detailed response by Matzke is in preparation; see also McDonald-Spicer et al. (2019).

Modifying standard biogeography models to create a trait-based dispersal model variant is conceptually simple (Sukumaran and Knowles 2018). First, the trait transition rate matrix is combined with the anagenetic geography rate matrix (Fig. 3A). Second, the number of possible cladogenetic range inheritance scenarios is doubled (Fig. 3B). As with standard biogeography models, the probability of any pair of descendant ranges after speciation, conditional on a particular ancestor state, is the weight of an individual cladogenesis scenario, divided by the total weight of all scenarios possible from that ancestral state. The main challenge is computational: Adding a binary trait doubles the size of the state space, and quadruples the size of the anagenetic rate matrix, resulting in slower computation of the matrix exponential in the likelihood calculation.

In order to estimate the likelihood of the combined trait and geography data under the assumption that traits and dispersal are independent, we ran the standard biogeographical models in BioGeoBEARS (DEC, DEC+$j$, DIVALIKE, DIVALIKE+$j$, BAYAREALIKE, BAYAREALIKE+$j$; Matzke 2013, 2014) without traits, and independently ran the trait data under binary discrete character models set up in BioGeoBEARS to make use of only the parameters $t_{12}$ and $t_{21}$. Adding the log-likelihoods of the geographic data and the trait data together produced the log-likelihood of the combined data under the trait-independent dispersal models. We compared the trait-independent models to trait-based dispersal models (DEC+$t_{12}+t_{21}+m_2$, DEC+$j+t_{12}+t_{21}+m_2$, DIVALIKE+$t_{12}+t_{21}+m_2$, DIVALIKE+$j+t_{12}+t_{21}+m_2$, BAYAREALIKE+$t_{12}+t_{21}+m_2$, BAYAREALIKE+$j+t_{12}+t_{21}+m_2$). In addition, we extended both trait-dependent and trait-independent models by the inclusion of geographical distance (+$x$ variants). The likelihood calculations of all traditional and new BioGeoBEARS models are checked in 156 unit tests (Cotton 2017) implemented with the R package testthat (Wickham 2011). The tests are available in the "tests" directory of the development version of BioGeoBEARS at https://github.com/nmatzke/BioGeoBEARS.

### Simulation-Inference Experiments

Simulation-inference tests are difficult for very large state spaces due to the slowness of the likelihood calculation, but we were able to run simulation-inference experiments for a system with 4 areas and a 2-state trait. We studied the reliability of inference of $m_2$ by performing 1200 simulation-inference runs under the DEC+$j+t_{12}+t_{21}+m_2$ model. The simulations simultaneously evolved the phylogenetic tree, the trait, and the biogeographic ranges of the lineages. We compared inference behavior for smaller and larger datasets (simulations stopped at 50 tips versus 150 tips), for different effect sizes ($m_2=1, 0.5$, or $0.125$, representing no effect, a moderate effect, and a large effect, respectively), and for models assuming a Yule phylogenetic process (the assumption made by DEC and related models; Matzke 2014) and a birth–death process with a large relative death rate inferred from an early draft of our dated phylogeny (birth rate $\lambda=0.091$, death rate $\mu=0.076$). Simulation-inference runs were also analyzed to measure how stochasticity in the counts of dispersal events within each trait state influenced the inference of $m_2$. The experiments are described in full in Supplemental Material available on Dryad.

### Paleogeographical Models

The trait-based model variant in BioGeoBEARS can be combined with time-stratified models (Ree and Smith 2008) where certain areas submerge in the past (Matzke 2014) or changes occur in the geographic distances between time strata (Van Dam and Matzke 2016). The 4 time-stratified model variants were: (i) changing distances, constant areas; (ii) changing distances, with New Caledonia submerged before 37 Ma; (iii) changing distances, with New Caledonia submerged between 52 and 37 Ma; and (iv) changing distances, with both New Caledonia and New Zealand submerged before 37 Ma.

### Optimization

Although successful optimization in a Maximum Likelihood search is typically trivial for the default BioGeoBEARS base models (which have only 2 or 3 free parameters), optimization can become more challenging when more parameters are added, even when it is ensured that they are formally identifiable. If a Maximum Likelihood search fails to find the parameter combination that actually maximizes the likelihood, then the subsequent model comparisons, likelihood ratio tests (LRT), etc., are invalid. We adopted (and recommend) the strategy of careful and critical inspection of optimization results, following the criteria laid out in the BioGeoBEARS online help pages (http://phylo.wikidot.com/biogeobears-mistakes-to-avoid#optim). The following steps helped to ensure optimization of more complex models. First, a slower, but more rigorous, optimization algorithm was used. The R package GenSA (Generalized Simulated Annealing; Xiang et al. 2013) performs more reliably than other commonly used optimizers (e.g., optim and optimx; Nash and Varadhan 2011) in higher-dimensional parameter spaces. In addition, GenSA has the useful feature that solutions can never have lower log-likelihood than the starting parameters (unfortunately,
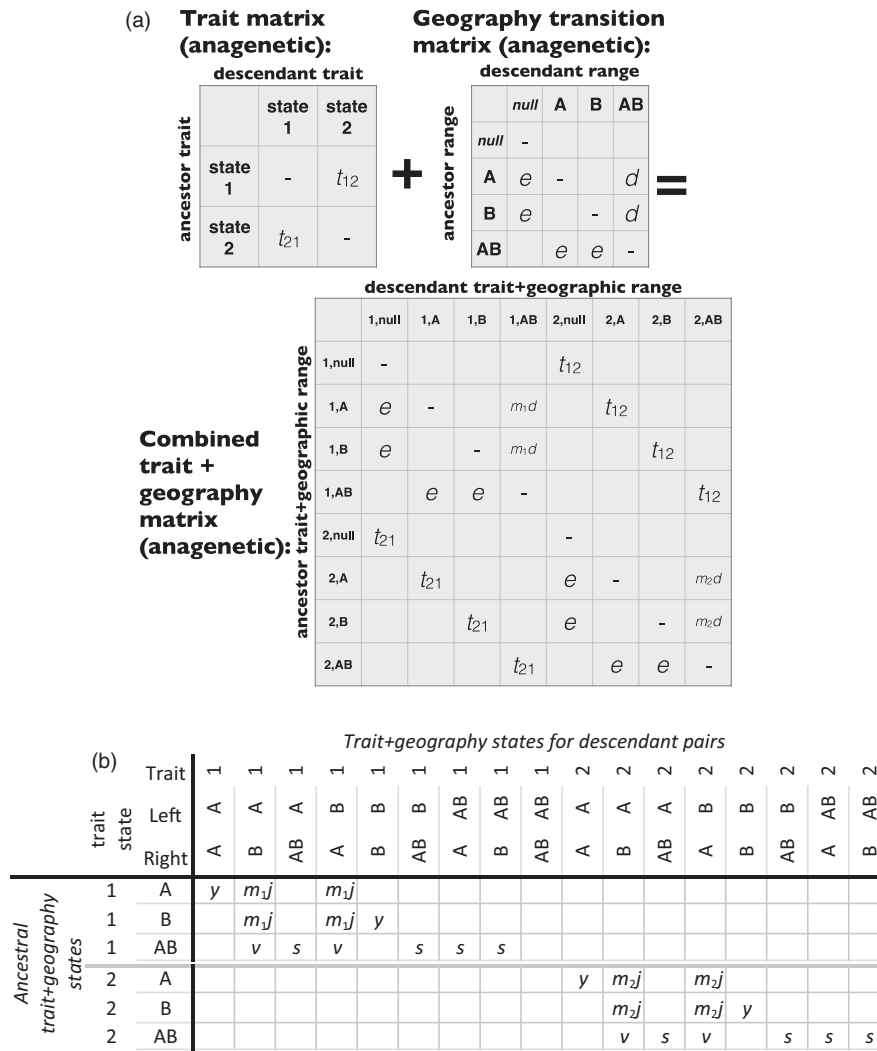
FIGURE 3.    Depiction of the anagenetic A) and cladogenetic B) transition matrices for a 2-state trait combined with biogeographical character with 2 areas (A and B) and thus 4 possible geographic ranges (null range, A, B, and AB). Real analyses would usually include more areas and thus many more possible geographic ranges, but the resulting matrices are too large to display graphically.

this is not a feature of optim and optimx). Second, model complexity was built up gradually, that is, the simplest models were run first, and then the ML parameters inferred from these runs were used as the starting values for the ML search in the next most complex model set. The most complex models can be reached through different pathways (e.g., Pathway 1: DEC → DEC+$j$ → DEC+$j$+$x$ → DEC+$j$+$x$ plus independent $t_{12}$+$t_{21}$ → DEC+$j$+$x$+$t_{12}$+$t_{21}$+$m_2$; Pathway 2: DEC → DEC+$x$ → plus independent $t_{12}$+$t_{21}$ → DEC+$x$+$t_{12}$+$t_{21}$+$m_2$ → DEC+$j$+$x$+$t_{12}$+$t_{21}$+$m_2$). Third, each of the trait-based models had its optimization re-run through the function "rerun_optimization_w_HiLow," which re-runs the optimization 3 times, starting at the original ML parameters, the parameters perturbed downwards, and the parameters perturbed upwards (the perturbation is user-specified; here, we used 25%). If the initial ML runs and re-runs produced different likelihoods, the models with the best likelihood were used to re-seed the search

and the runs and re-runs were repeated again until no further improvement was seen. An archive of data files and BioGeoBEARS code is available at the Dryad repository for this study.

### Statistical Model Comparison

Once we were satisfied with our ML optimizations, we used standard methods in statistical model comparison (Burnham and Anderson 2002) to judge the support our data gave to the various proposed models. Sample-size AICc was used to compare all 48 model variants together. While AICc does not provide frequentist $P$-values, it does provide a measure of relative model fit. AICc model weights (Burnham and Anderson 2002) were calculated for all models, and used to provide model-averaged estimates of key parameters. We also calculated LRT for nested pairs of models, but de-emphasize this

approach, as AICc represents a more appropriate statistical philosophy for comparing a variety of non-nested models, all of which are relatively simple compared with a very complex reality (Anderson and Burnham 2002; Anderson 2008).

## RESULTS

### Simulation-Inference Experiments

Results of the 1200 simulation-inference runs are shown in Figure 4. The results suggest that estimates of parameter $m_2$ cluster around the true simulation values, although with substantial scatter for smaller datasets. Adding lineage extinction to the simulations slightly increases the variance of estimates, but does not dramatically affect inference. For both Yule and Birth-Death simulations, the estimation error goes down as the dataset size increases. As expected, larger effect sizes (i.e., larger differences from the no-effect model, $m_2 = 1$) are easier to detect with small datasets, but weaker effects require larger datasets. For further details of simulation results, see Supplemental Material available on Dryad.

### Model Fits

The two best-fitting dispersal models for the combined trait and biogeography data of Podocarpaceae+Araucariaceae are the DIVALIKE+$j$+$x$+$t_{12}$+$t_{21}$+$m_2$ model with constant distances, with an AICc model weight of 58.8%, and the DIVALIKE+$j$+$x$+$t_{12}$+$t_{21}$+$m_2$ model with changing distances, with an AICc model weight of 15.4% (Table 1). Both of these models incorporate the dependence of dispersal rate on the morphological seed cone traits fleshy (F) and nonfleshy (N). Specifically, $m_2$, representing the multiplier on dispersal rate when a lineage has nonfleshy seed cones, is estimated to be 0.373 and 0.498 under these models. This suggests a substantial decrease in long-distance dispersal capability for Podocarpaceae with nonfleshy seeds.

The most-probable ranges under the best-fit model suggest that the ancestor of the family Podocarpaceae occupied the landmasses of today's Central- and South America (A) as well as Australia (G) and New Zealand (I) (AGI, Fig. 2). After a vicariance event, the ancestral range of the clade containing genera *Parasitaxus, Manoao, Lagarostrobos, Prumnopitys, Lepidothamnus, Halocarpus,* and *Phyllocladus* is estimated to be New Zealand (I), whereas the sister clade (containing genera *Saxegothaea, Microcachrys, Pherosphera, Acmopyle, Dacrycarpus, Falcatifolium, Dacrydium, Retrophyllum, Nageia, Afrocarpus,* and *Podocarpus*) is estimated to be on Central- and South America (A) and Australia (G).

Comparison of ancestral ranges (Table 2) resulting from the best model involving traits and constant geographical distances (DIVALIKE+$x$+$j$+$t_{12}$+$t_{21}$+$m_2$) and from the best model which does not involve traits but also relies on constant geographical distances (DEC+$x$+$j$+$t_{12}$+$t_{21}$) indicates that the inclusion of

traits results in different most-probable ancestral ranges for the ancestor of the family Araucariaceae, for the *Podocarpus* subgenus *Podocarpus* and for the genera *Nageia, Retrophyllum, Falcatifolium, Manoao, Lagarostrobos, Parasitaxus,* and *Lepidothamnus*. In all other clades and genera of the Podocarpaceae and Araucariaceae, both the trait-dependent and the trait-independent models suggest the same most-probable ranges. Table 2 shows the most likely ancestral range of each clade, together with divergence-time estimates.

### Seed Cone Evolution in Podocarpaceae

Fleshy cone structures appeared 7 times independently in the Podocarpaceae (Fig. 1): Within the genera *Parasitaxus, Manoao, Lagarostrobos, Lepidothamnus, Halocarpus,* and *Acmopyle,* and at the crown node of the clade which contains the genera *Podocarpus, Afrocarpus, Nageia, Retrophyllum, Dacrydium, Falcatifolium,* and *Dacrycarpus*. After the transformation back to nonfleshy seed cone structures in the clade containing *Retrophyllum, Nageia,* and *Afrocarpus*, seed cones of 2 species of the genus *Nageia* (*Nageia wallichiana* and *Nageia motley*) re-evolved the fleshy and bird-attracting trait. Except for the *Retrophyllum*+*Nageia*+*Afrocarpus* clade, reversion to the original trait of nonfleshy cones was only observed in a small clade containing the African and Madagascan *Podocarpus* species.

### Statistical Model Comparison

Across all 48 models, model variants that included distance-dependent dispersal (+$x$) and founder-event jump dispersal (+$j$) accrued 100% of the AICc model weight. Trait-dependent model variants together earned 87.5% of the AICc model weight (Table 1). The rest of the model weight was taken up by the distance-dependent but trait-independent models DEC+$x$+$j$+$t_{12}$+$t_{21}$, (8.6%) and DIVALIKE+$x$+$j$+$t_{12}$+$t_{21}$ (3.9%), indicating that these are also credible (Burnham et al. 2011). LRTs on pairs of models show that adding the parameters $x$ and $j$ results in statistically significantly higher likelihood values in all compared model pairs. Adding the parameter $m_2$, the trait-dependent dispersal multiplier, significantly increased the likelihood of the data over the DIVALIKE+$j$+$x$+$t_{12}$+$t_{21}$ model (P-value 0.006), but not for the DEC+$j$+$x$ model (P = 0.196). These results suggest that the choice of base biogeographical model may be important for detecting trait-dependent dispersal in this dataset.

Comparing constant geography and time-stratified models, the AICc weights indicate that the best-fitting category of models assume constant geological distances over time with a combined model weight of 78.0% (Table 1). Models with changing distances are not only weaker fits, but also credible (21.9% AICc model weight). However, models that include the submergence of New Caledonia or the simultaneous submergence of New

TABLE 1. Testing for the influence of trait state, distance, and changing geography on dispersal rates

| Model category | Time-stratification | Base model | np | geog lnL | trait lnL | joint lnL | $d$ | $e$ | $j$ | $x$ | $t_{12}$ | $t_{21}$ | $m_1$ | $m_2$ | AICc weight | adding $j$ P-value | adding $x$ P-value | adding $m_2$ P-value |
|---|---|---|---|---|---|---|---|---|---|---|---|---|---|---|---|---|---|---|
| Distance-indep. trait-indep. | Constant geography | DEC+$t_{12}$+$t_{21}$ | 4 | −427.11 | −25.1 | −452.2 | 0.0049 | 0.0072 | 0 | 0 | 0.0054 | 0.0016 | 1 | 1 | 0.0% | | | |
| | | DEC+$j$+$t_{12}$+$t_{21}$ | 5 | −416.15 | −25.1 | −441.2 | 0.0024 | 9E-07 | 0.015 | 0 | 0.0054 | 0.0016 | 1 | 1 | 0.0% | 2.8E-06*** | | |
| | | DIVALIKE+$t_{12}$+$t_{21}$ | 4 | −450.85 | −25.1 | −475.9 | 0.0064 | 0.0087 | 0 | 0 | 0.0054 | 0.0016 | 1 | 1 | 0.0% | | | |
| | | DIVALIKE+$j$+$t_{12}$+$t_{21}$ | 5 | −424.93 | −25.1 | −450.0 | 0.0027 | 1E-06 | 0.016 | 0 | 0.0054 | 0.0016 | 1 | 1 | 0.0% | 6.0E-13*** | | |
| | | BAYAREALIKE+$t_{12}$+$t_{21}$ | 4 | −535.53 | −25.1 | −560.6 | 0.01 | 0.0555 | 0 | 0 | 0.0054 | 0.0016 | 1 | 1 | 0.0% | | | |
| | | BAYAREALIKE+$j$+$t_{12}$+$t_{21}$ | 5 | −440.95 | −25.1 | −466.0 | 0.0014 | 0.0081 | 0.026 | 0 | 0.0054 | 0.0016 | 1 | 1 | 0.0% | 4.8E-43*** | | |
| Distance-indep. trait-dep. | Constant geography | DEC+$t_{12}$+$t_{21}$+$m_2$ | 5 | | | −450.1 | 0.006 | 0.004 | 0 | 0 | 0.0037 | 0.0044 | 1 | 0.419 | 0.0% | | | 0.041* |
| | | DEC+$j$+$t_{12}$+$t_{21}$+$m_2$ | 6 | | | −439.8 | 0.003 | 0.000 | 0.017 | 0 | 0.0034 | 0.0044 | 1 | 0.528 | 0.0% | 5.6E-06*** | | 0.091ns |
| | | DIVALIKE+$t_{12}$+$t_{21}$+$m_2$ | 5 | | | −468.1 | 0.009 | 0.000 | 0 | 0 | 0.0035 | 0.0048 | 1 | 0.279 | 0.0% | | | 7.2E-05*** |
| | | DIVALIKE+$j$+$t_{12}$+$t_{21}$+$m_2$ | 6 | | | −446.0 | 0.004 | 0.000 | 0.019 | 0 | 0.0035 | 0.0044 | 1 | 0.404 | 0.0% | 3.2E-11*** | | 0.005** |
| | | BAYAREALIKE+$t_{12}$+$t_{21}$+$m_2$ | 5 | | | −559.7 | 0.012 | 0.055 | 0 | 0 | 0.0054 | 0.0013 | 1 | 0.698 | 0.0% | | | 0.177ns |
| | | BAYAREALIKE+$j$+$t_{12}$+$t_{21}$+$m_2$ | 6 | | | −465.9 | 0.001 | 0.008 | 0.027 | 0 | 0.0054 | 0.0016 | 1 | 0.866 | 0.0% | 1.1E-42*** | | 0.618ns |
| Distance-dep. trait-indep. | Constant geography | DEC+$x$+$t_{12}$+$t_{21}$ | 5 | −398.13 | −25.1 | −423.2 | 0.0692 | 0.0069 | 0 | −0.87 | 0.0054 | 0.0016 | 1 | 1 | 0.0% | | 3E-14*** | |
| | | DEC+$x$+$j$+$t_{12}$+$t_{21}$ | 6 | −384.42 | −25.1 | −409.5 | 0.030 | 3E-07 | 0.287 | −0.88 | 0.0054 | 0.0016 | 1 | 1 | 8.6% | 0.000*** | 2E-15*** | |
| | | DIVALIKE+$x$+$t_{12}$+$t_{21}$ | 5 | −409.14 | −25.1 | −434.2 | 0.1071 | 0.0064 | 0 | −0.96 | 0.0054 | 0.0016 | 1 | 1 | 0.0% | | 7E-20*** | |
| | | DIVALIKE+$x$+$j$+$t_{12}$+$t_{21}$ | 6 | −385.22 | −25.1 | −410.3 | 0.0338 | 1E-07 | 0.210 | −0.84 | 0.0054 | 0.0016 | 1 | 1 | 3.9% | 0.000*** | 5E-19*** | |
| | | BAYAREALIKE+$x$+$t_{12}$+$t_{21}$ | 5 | −511.0 | −25.1 | −536.1 | 0.1186 | 0.058 | 0 | −0.79 | 0.0054 | 0.0013 | 1 | 1 | 0.0% | | 2E-12*** | |
| | | BAYAREALIKE+$x$+$j$+$t_{12}$+$t_{21}$ | 6 | −405.85 | −25.1 | −430.9 | 0.020 | 0.004 | 0.330 | −0.87 | 0.0054 | 0.0016 | 1 | 1 | 0.0% | 1.2E-47*** | 5E-17*** | |
| Distance-dep. trait-dep. | Constant geography | DEC+$x$+$t_{12}$+$t_{21}$+$m_2$ | 6 | | | −421.5 | 0.086 | 0.007 | 0 | −0.88 | 0.0057 | 0.0014 | 1 | 0.575 | 0.0% | | 4E-14*** | 0.066ns |
| | | DEC+$x$+$j$+$t_{12}$+$t_{21}$+$m_2$ | 7 | | | −408.7 | 0.048 | 0.000 | 0.404 | −0.93 | 0.0028 | 0.0040 | 1 | 0.590 | 6.8% | 4.0E-07*** | 2E-14*** | 0.196ns |
| | | DIVALIKE+$x$+$t_{12}$+$t_{21}$+$m_2$ | 6 | | | −429.6 | 0.139 | 0.004 | 0 | −0.92 | 0.0035 | 0.0048 | 1 | 0.367 | 0.0% | | 2E-18*** | 0.002** |
| | | DIVALIKE+$x$+$j$+$t_{12}$+$t_{21}$+$m_2$ | 7 | | | −406.5 | 0.063 | 0.000 | 0.273 | −0.86 | 0.0044 | 0.0051 | 1 | 0.373 | 58.8% | 1.1E-11*** | 6E-18*** | 0.006** |
| | | BAYAREALIKE+$x$+$t_{12}$+$t_{21}$+$m_2$ | 6 | | | −535.0 | 0.137 | 0.058 | 0 | −0.78 | 0.0054 | 0.0013 | 1 | 0.683 | 0.0% | | 2E-12*** | 0.141ns |
| | | BAYAREALIKE+$x$+$j$+$t_{12}$+$t_{21}$+$m_2$ | 7 | | | −430.0 | 0.026 | 0.003 | 0.408 | −0.91 | 0.0055 | 0.0016 | 1 | 0.640 | 0.0% | 1.4E-47*** | 2E-17*** | 0.161ns |
| Distance-dep. trait-dep. | Changing distances, all areas extant | DEC+$x$+$t_{12}$+$t_{21}$+$m_2$ | 6 | | | −421.2 | 0.089 | 0.007 | 0 | −0.88 | 0.0058 | 0.0013 | 1 | 0.522 | 0.0% | | 3E-14*** | |
| | | DEC+$x$+$j$+$t_{12}$+$t_{21}$+$m_2$ | 7 | | | −408.7 | 0.037 | 0.000 | 0.279 | −0.82 | 0.0039 | 0.0040 | 1 | 0.486 | 6.5% | 5.7E-07*** | 2E-14*** | |
| | | DIVALIKE+$x$+$t_{12}$+$t_{21}$+$m_2$ | 6 | | | −429.6 | 0.139 | 0.005 | 0 | −0.92 | 0.0035 | 0.0047 | 1 | 0.389 | 0.0% | | 2E-18*** | |
| | | DIVALIKE+$x$+$j$+$t_{12}$+$t_{21}$+$m_2$ | 7 | | | −407.8 | 0.046 | 0.000 | 0.241 | −0.80 | 0.0071 | 0.0054 | 1 | 0.498 | 15.4% | 4.5E-11*** | 2E-18*** | |
| | | BAYAREALIKE+$x$+$t_{12}$+$t_{21}$+$m_2$ | 6 | | | −534.4 | 0.147 | 0.059 | 0 | −0.81 | 0.0054 | 0.0013 | 1 | 0.677 | 0.0% | | 1E-12*** | |
| | | BAYAREALIKE+$x$+$j$+$t_{12}$+$t_{21}$+$m_2$ | 7 | | | −430.3 | 0.025 | 0.004 | 0.372 | −0.88 | 0.0055 | 0.0016 | 1 | 0.650 | 0.0% | 3.1E-47*** | 2E-17*** | |
| Distance-dep. trait-dep. | Changing distances, New Caledonia rises at 37 Ma | DEC+$x$+$t_{12}$+$t_{21}$+$m_2$ | 6 | | | −425.7 | 0.084 | 0.008 | 0 | −0.85 | 0.0057 | 0.0013 | 1 | 0.556 | 0.0% | | | |
| | | DEC+$x$+$j$+$t_{12}$+$t_{21}$+$m_2$ | 7 | | | −413.9 | 0.041 | 0.002 | 0.266 | −0.81 | 0.0040 | 0.0040 | 1 | 0.567 | 0.0% | 1.2E-06*** | | |
| | | DIVALIKE+$x$+$t_{12}$+$t_{21}$+$m_2$ | 6 | | | −434.0 | 0.140 | 0.006 | 0 | −0.91 | 0.0036 | 0.0046 | 1 | 0.403 | 0.0% | | | |
| | | DIVALIKE+$x$+$j$+$t_{12}$+$t_{21}$+$m_2$ | 7 | | | −413.6 | 0.058 | 0.000 | 0.247 | −0.84 | 0.0031 | 0.0045 | 1 | 0.457 | 0.0% | 1.8E-10*** | | |
| | | BAYAREALIKE+$x$+$t_{12}$+$t_{21}$+$m_2$ | 6 | | | −536.8 | 0.158 | 0.060 | 0 | −0.83 | 0.0054 | 0.0013 | 1 | 0.678 | 0.0% | | | |
| | | BAYAREALIKE+$x$+$j$+$t_{12}$+$t_{21}$+$m_2$ | 7 | | | −432.4 | 0.027 | 0.005 | 0.360 | −0.87 | 0.0056 | 0.0015 | 1 | 0.623 | 0.0% | 2.4E-47*** | | |
| Distance-dep. trait-dep. | Changing New Caledonia+ New Zealand rise at 37 Ma | DEC+$x$+$t_{12}$+$t_{21}$+$m_2$ | 6 | | | −436.4 | 0.082 | 0.014 | 0 | −0.74 | 0.0057 | 0.0011 | 1 | 0.522 | 0.0% | | | |
| | | DEC+$x$+$j$+$t_{12}$+$t_{21}$+$m_2$ | 7 | | | −429.6 | 0.050 | 0.009 | 0.161 | −0.73 | 0.0056 | 0.0012 | 1 | 0.572 | 0.0% | 0.000*** | | |
| | | DIVALIKE+$x$+$t_{12}$+$t_{21}$+$m_2$ | 6 | | | −446.5 | 0.130 | 0.015 | 0 | −0.81 | 0.0056 | 0.0013 | 1 | 0.479 | 0.0% | | | |
| | | DIVALIKE+$x$+$j$+$t_{12}$+$t_{21}$+$m_2$ | 7 | | | −432.2 | 0.072 | 0.009 | 0.191 | −0.80 | 0.0056 | 0.0013 | 1 | 0.514 | 0.0% | 0.000*** | | |
| | | BAYAREALIKE+$x$+$t_{12}$+$t_{21}$+$m_2$ | 6 | | | −539.4 | 0.173 | 0.062 | 0 | −0.85 | 0.0054 | 0.0013 | 1 | 0.672 | 0.0% | | | |
| | | BAYAREALIKE+$x$+$j$+$t_{12}$+$t_{21}$+$m_2$ | 7 | | | −446.7 | 0.030 | 0.012 | 0.279 | −0.78 | 0.0055 | 0.0014 | 1 | 0.642 | 0.0% | 3.2E-42*** | | |
| Distance-dep. trait-dep. | Changing distances, New Caledonia sunken from 52-37 Ma | DEC+$x$+$t_{12}$+$t_{21}$+$m_2$ | 6 | | | −428.0 | 0.084 | 0.008 | 0 | −0.86 | 0.0056 | 0.0015 | 1 | 0.575 | 0.0% | | | |
| | | DEC+$x$+$j$+$t_{12}$+$t_{21}$+$m_2$ | 7 | | | −415.6 | 0.041 | 0.002 | 0.277 | −0.82 | 0.0033 | 0.0044 | 1 | 0.525 | 0.0% | 6.0E-07*** | | |
| | | DIVALIKE+$x$+$t_{12}$+$t_{21}$+$m_2$ | 6 | | | −436.1 | 0.141 | 0.006 | 0 | −0.92 | 0.0034 | 0.0048 | 1 | 0.384 | 0.0% | | | |
| | | DIVALIKE+$x$+$j$+$t_{12}$+$t_{21}$+$m_2$ | 7 | | | −415.5 | 0.060 | 0.000 | 0.271 | −0.86 | 0.0030 | 0.0046 | 1 | 0.446 | 0.0% | 1.3E10*** | | |
| | | BAYAREALIKE+$x$+$t_{12}$+$t_{21}$+$m_2$ | 6 | | | −538.6 | 0.155 | 0.060 | 0 | −0.83 | 0.0055 | 0.0013 | 1 | 0.706 | 0.0% | | | |
| | | BAYAREALIKE+$x$+$j$+$t_{12}$+$t_{21}$+$m_2$ | 7 | | | −434.0 | 0.028 | 0.005 | 0.375 | −0.88 | 0.0055 | 0.0016 | 1 | 0.593 | 0.0% | 2.6E-43*** | | |

Notes: For the LRT for adding single parameters, ***, **, and * indicate significance at P-value cutoffs 0.001, 0.01, and 0.05, respectively. "ns" indicates "nonsignificant" at the 0.05 cutoff.
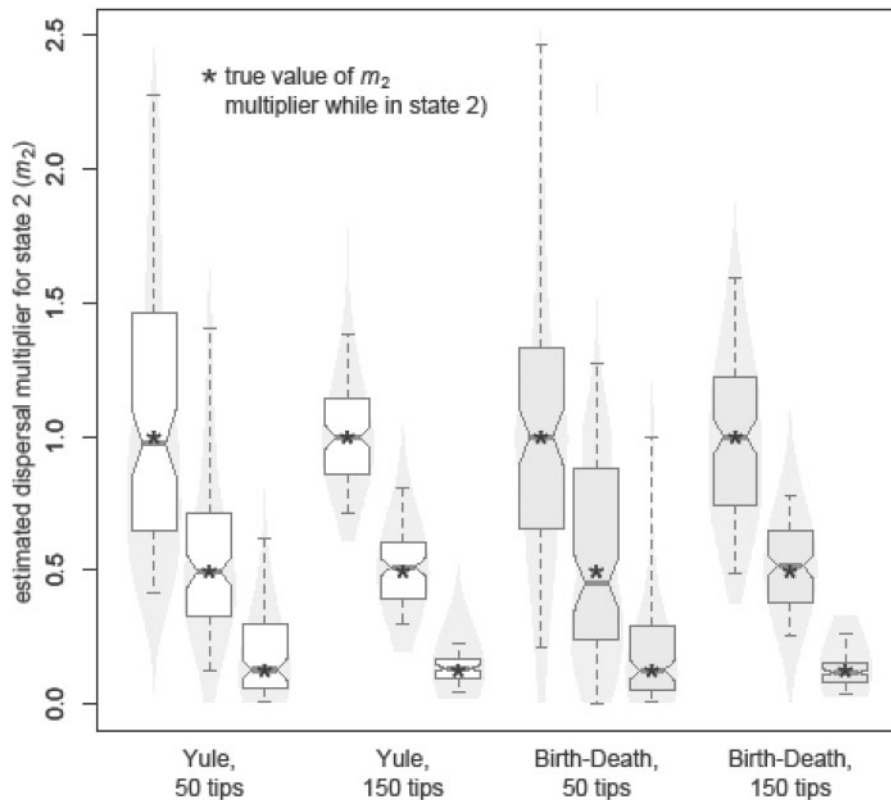
FIGURE 4. Inference of the key parameter, $m_2$ (the dispersal multiplier when a lineage is in trait state 2), on simulated data. The true value of $m_2$ used in the simulations is indicated by *. Each simulation simultaneously evolved the phylogenetic tree, trait data, and biogeographic range data. Boxes show the middle quartiles and median of estimates, whiskers the 10th and 90th percentiles. White boxplots indicate that the simulations used a Yule process (pure birth) assumption; Grey boxplots indicate a birth–death process (parameters described in text). Violin plots were added with the vioplot R package (Adler 2015). A total of 100 simulation-inference runs were done for each combination of parameters and dataset size, for a total of 1200.

Caledonia and New Zealand have small weight (0.01% total).

## DISCUSSION

Our analyses suggest that models where dispersal is dependent on seed cone fleshiness and geographical distance are better fits to the data than models where dispersal is independent of traits and/or distances. In the best-fitting model (DIVALIKE+$j$+$x$+$t_{12}$+$t_{21}$+$m_2$), an estimated $m_2$ of 0.37 suggests that macroevolutionary dispersal rates are 63% lower for lineages with nonfleshy cones. Even when $m_2$ is estimated from a weighted average of all 48 models, the model-averaged estimate of $m_2 = 0.49$ suggests a dispersal rate 51% lower for nonfleshy cones. An estimated $x$ of $-0.86$ under the best model (the model-averaged estimate is very similar, $-0.856$) suggests a strong negative correlation between dispersal and increasing distance (an $x$ of $-1$ indicates a linear relationship between inverse distance and dispersal probability, that is, doubling the distance halves the dispersal probability). A possible explanation of these results is that seed dispersal between more distant areas is increasingly restricted due gut passage times in birds (Weir and Corlett 2007).

Model comparisons among time-stratified models representing different scenarios (Table 1), revealed that models which assume a total submergence of New Caledonia (with or without the submergence of New Zealand) are not favored in explaining the dispersal history of the Podocarpaceae. According to our results, it is more likely that at least parts of these islands have served as Gondwanan refugia. This finding agrees with some previous work (e.g. Lowry 1998; Murienne et al. 2005). Other studies, however, suggested that the colonization of New Caledonia must be the result of recent long-distance dispersal events and that the diversity of this island results from recent radiations (e.g. Grandcolas et al. 2008; Swenson et al. 2014). We suggest that comparing models allowing for the permanent existence of New Caledonia against models including a temporary submergence could be an important step in weighing the evidence provided by different plant groups.

### Historical Biogeography of the Podocarpaceae

Estimation of ancestral ranges under the best-fit model (DIVALIKE+$j$+$x$+$t_{12}$+$t_{21}$+$m_2$) suggests that Podocarpaceae originated on the landmasses of today's

TABLE 2. Bayesian posterior divergence-time estimates (Median and 95% highest posterior density) for the main clades and genera of the Podocarpaceae and Araucariaceae, along with the most-probable ancestral trait states and ancestral ranges

| Clade/genus | Stem group age in MA (95% HPI) | Crown group age in MA (95% HPI) | Seed cone type | Ancestral ranges trait-dependent model (DIVALIKE+$j$+$x$+ $t_{12}$+$t_{21}$+$m_2$) | Ancestral ranges trait-independent model (DEC+$j$+$x$) |
|---|---|---|---|---|---|
| Podocarpaceae | 185.3 (171.4–215.1) | 130.2 (100.2–159.3) | FN | AGI (67%) | AGI (51%) |
| *Podocarpus* | 39.8 (28.3–52.5) | 25.5 (17.3–35.3) | F* | G (45%) | G (32%) |
| *Podocarpus* subg. *Podocarpus* | 25.5 (17.3–35.3) | 17.5 (11.5–23.9) | F* | AG (39%) | G (47%) |
| *Podocarpus* subg. *Foliolatus* | 25.5 (17.3–35.3) | 11.24 (7.4–15.6) | F | G (27%) | G (28%) |
| *Nageia* | 16.8 (10.1–24.5) | 7.2 (4–10.8) | N* | C (75%) | CD (30.1%) |
| *Afrocarpus* | 16.8 (10.1–24.5) | 3.5 (0.7–8.5) | N | B (100%) | B (100%) |
| *Retrophyllum* | 28.6 (19.5–39.5) | 11 (5.6–17) | N | AEH (12%) | AH (9%) |
| *Dacrydium* | 24.6 (15.5–34.8) | 12.7 (7.9–18.1) | F | D (43%) | DEH (21%) |
| *Falcatifolium* | 24.6 (15.5–34.8) | 15.1 (7.7–23.5) | F | EH (35%) | H (46%) |
| *Dacrycarpus* | 54.8 (50.6–59.9) | 8.14 (4.2–13.3) | F | EHI (57%) | EHI (34%) |
| *Acmopyle* | 82.4 (65.5–101) | 26.9 (12.2–45) | F | FH (79%) | FH (50%) |
| *Pherosphera* | 92.3 (73.3–115.2) | 4.6 (0.8–10) | N | G (100%) | G (100%) |
| *Microcachrys* | 101.4 78.7–125.9 | — | N | G (89%) | G (66%) |
| *Saxegothaea* | 111.6 (86–138.6) | — | N | AG (82%) | AG (54%) |
| *Prumnopitys* | 93.2 (65.5–123.2) | 56.8 (36.6–80.4) | N | I (66%) | I (49%) |
| *Manoao* | 60.6 (35.9–88.9) | — | F | GI (62%) | I (64%) |
| *Lagarostrobos* | 60.6 (35.9–88.9) | — | F | GI (62%) | I (64%) |
| *Parasitaxus* | 80 (50.6–106.7) | — | F | HI (43%) | I (58%) |
| *Phyllocladus* | 64.2 (48.9–86.2) | 6.9 (2.8–11.6) | N | I (99%) | I (82%) |
| *Halocarpus* | 88.7 (62.7–118.3) | 4 (1–8) | F | I (100%) | I (100%) |
| *Lepidothamnus* | 64.2 (48.9–86.2) | 14 (6.3–23.8) | F | AI (76%) | I (51%) |
| Araucariaceae | 185.3 (171.4–215.1) | 54.4 (37–73) | N | EGH (27%) | GHI (25%) |
| *Araucaria* | 54.4 (37–72.9) | 40.3 (24.5–56.7) | N | G (27%) | G (43%) |
| *Agathis* | 39.8 (26.6–54.6) | 32.1 (21.1–44.6) | N | HI (22%) | HI (16%) |
| *Wollemia* | 39.8 (26.6–54.6) | — | N | G (21%) | G (27%) |

Note: Seed cone type: F = red or black fleshy cone structures and a fleshy receptaculum, N = seed cone structures coriaceous (non-fleshy), no receptaculum, *Seed cone type F only in two species of *Nageia: Nageia motleyi* and *Nageia wallichiana*; Seed cone type N only in the *Podocarpus* species from Africa and Madagascar; Ancestral ranges resulting from the trait-dependent model DIVALIKE+$j$+$x$+$t_{12}$+$t_{21}$+$m_2$ and the trait-independent model DEC+$j$+$x$.

Central- and South America (A), Australia (G), and New Zealand (I) in the Early Jurassic (185.3 Ma). Brodribb and Hill (1999) reported possible Podocarpaceae macrofossils from the Early Triassic, suggesting that the family originated some time earlier. However, these Triassic Podocarpaceae fossils, like *Notophytum krauselii* described by Meyer-Berthaud and Taylor (1991), are controversial and not commonly accepted as members of this family (Leslie et al. 2012). Early unequivocal fossils of the Podocarpaceae are the Early Cretaceous *Squamastrobus tigrensis* (Archangelsky and Del Fueyo 1989) from Patagonia and *Bellarinea barklyi* (Drinnan and Chambers 1986) from south-eastern Australia, concordant with the estimated ancestral range of the Podocarpaceae from our analysis. We can compare our results to the studies of Wagstaff (2004) on the genus *Phyllocladus* and Quiroga et al. (2016) on the genus *Podocarpus*. Wagstaff (2004) compiled Tertiary fossil localities of *Phyllocladus*, which are all known from Australia and New Zealand. Our analysis (best model) revealed an origin of *Phyllocladus* on New Zealand (I). This may indicate that there would be a benefit to including fossil taxa in phylogenetic biogeography analyses, at least if they can be placed fairly confidently in a dated phylogeny. The results of Quiroga et al. (2016) suggest that the ancestral range of the *Podocarpus* subgenus *Foliolatus* was restricted to East

Gondwana, and that the ancestral range of subgenus *Podocarpus* was West Gondwana. In contrast, our analysis suggested the ancestral range of subgenus *Foliolatus* was Australia and of the subgenus *Podocarpus* to be on the landmasses of today's America and Australia. The more widespread ancestor inferred by Quiroga et al. (2016) is probably due to a combination of the DEC model, the coarser areas used, and the lack of outgroups to *Podocarpus* in their biogeographic analysis.

### Seed Cone Evolution in Podocarpaceae

According to our analyses (all models), the earliest transition from nonfleshy to fleshy seed cones within the Podocarpaceae took place in the Late Cretaceous (~82.4 Ma). This happened at the base of the clade which contains *Podocarpus, Afrocarpus, Nageia, Retrophyllum, Dacrydium, Falcatifolium*, and *Dacrycarpus* (Fig. 1). This trend reflects the main distribution strategy (endozoochory by birds) of the Podocarpaceae in recent times. The appearance of fleshy seed cones may be correlated with the early diversification of birds, which also took place in the Late Cretaceous (~70–80 Ma). This was later followed by an explosive radiation of crown birds together with a radiation of fruit-eating clades in the wake of the Cretaceous-Paleogene (K-Pg) mass

extinction (e.g., Coraciimorphae ~48–66 Ma; see Prum et al. 2015; Viseshakul et al. 2011).

The reversion of the *Retrophyllum+Nageia+Afrocarpus* clade to the ancestral trait of non-fleshy seed cones took place by the Early Eocene, an epoch characterized by increasing temperatures and decreasing, more seasonal rainfall (e.g. Rea et al. 1990; Zachos et al. 2008; Hansen et al. 2013). Evolution of nonfleshiness could be a response to limited water availability. Other adaptations to drier conditions, such as the loss of stomata or the reduction of leave size, were recorded for several fossil podocarp genera during the same time period (Hill 1995). The reversion to nonfleshy seed cone structures also took place in a small clade, which includes all African and Madagascan Podocarpaceae, by the beginning of the Miocene. Because there is no evidence for similar climate change in this case (Miocene climate in Africa is characterized by a higher humidity than today), other limiting factors must have played a role, such as adaptations to different seed dispersal modes (e.g. Guimarães et al. 2008).

### *Limitations of Current Models and Suggestions for Improvement*

We view our models as steps forward in explaining the geographic distribution of Podocarpaceae, as well as the evolution of their seed cone traits, and how traits and dispersal are linked. We suggest that the framework of statistical model comparison is a productive one because it provides explicit tests of model fit, and a quantitative measure of how strongly the data support various models. We acknowledge that the presently available models have several limitations. One is uncertainty in geological history. Estimates of paleo-distances depend on plate tectonics models, as well as the timing and completeness of submergence of, for example, parts of Zealandia (Mortimer et al. 2017). Although estimates of paleo-distances are likely to be fairly well correlated despite the details of plate tectonics and coastline models, any complete submergence events could have dramatic impacts on biogeographic history. However, finding statistical support for complete submergence events in BioGeoBEARS analyses might be challenging, even if the events are real. Within the BioGeoBEARS framework, time-stratified models with dramatic changes in geography (submerging areas, or strong statements of connectivity/disconnectivity) are only likely to improve the data likelihood if the dating of the proposed geological scenario and the phylogenetic dating of the relevant clades matches well. An MCC phylogeny from a BEAST analysis, and a geological scenario, both represent point estimates of history. It is appealing to consider the possibility of jointly sampling geological and phylogenetic dating histories via Bayesian methods; steps in this direction are taken by Landis (2016) and Landis et al. (2018). However, the slowness of the likelihood calculation for the large state spaces required by traits-based dispersal models is likely to remain a challenge for fully Bayesian methods. Other methods, such as those based on classification of an empirical dataset against simulations under different models (e.g. Sukumaran et al. 2016), may be useful in situations where fully likelihood calculations are impractical. However, these may come at the cost of some of the useful by-products of likelihood methods, such as explicit estimates of parameters and ancestral range probabilities under each model, and use of simple methods for statistical model comparison (Burnham and Anderson 2002).

More fundamentally, there has been little study of how large a phylogenetic dataset it would take to begin to influence geological reconstructions. Inclusion of fossils in phylogenies (Bapst et al. 2016; Matzke and Wright 2016), and fitting models to the phylogenies of many clades simultaneously, may provide some paths forward. Perhaps the most fundamental limitation of all of the models considered here is that they leave out the process of lineage extinction (Marshall 2017). Extinction certainly is an important process in a clade like Podocarpaceae, and models that can include extinction as a process exist, namely the state-dependent speciation and extinction "SSE" models (Fitzjohn 2010, 2012; Goldberg et al. 2011; Goldberg and Igic 2012; Magnuson-Ford and Otto 2012). However, the efficient calculation of data likelihoods under SSE models for the very large state spaces necessary for linking traits to complex geography models appears difficult at present. We can gain some confidence from the fact that in the Podocarpaceae, traits and geographic ranges are observably conserved along the phylogeny. It is therefore likely that the speciation/extinction process has not totally obscured the phylogenetic signal in the distribution of geographic ranges and traits at the tips of the tree, supporting the potential to detect correlations between dispersal and trait states.

One final limitation of the trait-based dispersal model considered here is that it may be subject to criticisms similar to those aimed at models that examine the correlation between 2 discrete traits (Maddison and Fitzjohn 2015; Uyeda et al. 2018). Observed correlation between a trait and dispersal rate does not prove that the examined trait is the causal agent in increasing or decreasing dispersal. Instead, any other trait with a similar distribution on the phylogeny might be the cause (Uyeda et al. 2018). In addition, it is possible that dispersal rates could vary across a phylogeny for reasons unrelated to a trait under study, but a trait-dependent model nevertheless better captures this variation and so increases model fit (Caetano et al. 2018). Caetano et al. (2018) address this with their GeoHiSSE model, although this solution will share the computational speed limitations of other SSE models. These issues should be ameliorated somewhat in a dataset such as ours, where many transitions in the seed trait are observed, and dispersal events occur throughout the tree.

The above issues are a reminder that statistical model comparison is a tool to be used with "a considerable amount of careful, a priori thinking in arriving at

a set of candidate models," "keeping the number of candidate models small," with researcher experience ensuring models are "well-founded" (Burnham and Anderson 2002, pp. 17, 18). For this reason, we would not recommend using trait-based dispersal models for untargeted "fishing expeditions," where dozens or hundreds of traits are tested for their "influence" on dispersal rate. Such a study would have a high chance of yielding misleading results (Anderson 2008).

## SUPPLEMENTARY MATERIAL

Data available from the Dryad Digital Repository: https://doi.org/10.5061/dryad.d117b3k.

## REFERENCES

Adler D. 2015. Package 'vioplot', R package version 0.2. Available from: URL https://cran.r-project.org/web/packages/vioplot/vioplot.pdf.

Anderson D.R. 2008. Model based inference in the life sciences: a primer on evidence. New York (NY): Springer.

Anderson, D.R., Burnham, K.P. 2002. Avoiding pitfalls when using information-theoretic methods. J. Wildl. Manage. 66(3):912–918.

Archangelsky S., Del Fueyo G.M. 1989. *Squamastrobus* gen. n., a fertile podocarp from the early Cretaceous of Patagonia, Argentina. Rev. Palaeobot. Palyn. 59:109–126.

Baker H.G. 1955. Self-compatibility and establishment after 'long distance' dispersal. Evolution 9:347–348.

Bapst D.W., Wright A.M., Matzke N.J., Lloyd G.T. 2016. Topology, divergence dates, and macroevolutionary inferences vary between different tip-dating approaches applied to fossil theropods (Dinosauria). Biol. Lett. 12:20160237.

Bouckaert R., Heled J., Kuhnert D., Vaughan T., Wu C.-H., Xie D., Suchard M.A., Rambaut A., Drummond A.J. 2014. BEAST 2: a software platform for Bayesian evolutionary analysis. PLoS Comp. Biol. 10:e1003537.

Brodribb T.J., Hill R.S. 1999. Southern conifers in time and space. Aust. J. Bot. 47:639–696.

Burnham K.P., Anderson D.R. 2002. Model selection and multimodel inference—a practical information-theoretic approach. New York: Springer.

Burnham, K.P., Anderson, D.R., Huyvaert, K.P. 2011. AIC model selection and multimodel inference in behavioral ecology: some background, observations, and comparisons. Behav. Ecol. Sociobiol. 65(1):23–35.

Caetano, D.S., O'Meara, B.C., Beaulieu, J.M. 2018. Hidden state models improve statedependent diversification approaches, including biogeographical models. Evolution 72:2308–2324.

Carlquist S.J. 1965. Island life: a natural history of the islands of the world. New York (NY): Natural History Press.

Cotton, R. 2017. Testing R Code, 1st ed. Cambridge, Massachusetts: Chapman & Hall/CRC The R Series.

Darwin C. 1859. On the origin of species by means of natural selection, or the preservation of favoured races in the struggle for life. London: John Murray.

de Queiroz A. 2014. The monkey's voyage: How improbable journeys shaped the history of life. New York (NY): Basic Books.

Drinnan A.N., Chambers T.C. 1986. Flora of the Lower Cretaceous Koonwarra fossil bed (Korumburra group), South Gippsland, Victoria. In: Jell P.A., Roberts J., editors. Plants and invertebrates from the Lower Cretaceous Koonwarra fossil bed, South Gippsland, Victoria. Sydney: Association of Australasian Palaeontologists. p. 77.

Eriksson O. 2008. Evolution of seed size and biotic seed dispersal in angiosperms: paleoecological and neoecological evidence. Int. J. Pl. Sci. 169:863–870.

Farjon A. 2010. A handbook of the world's conifers. Leiden: Brill.

Fitzjohn R.G. 2010. Quantitative traits and diversification. Syst. Biol. 59:619–633.

Fitzjohn R.G. 2012. Diversitree: comparative phylogenetic analyses of diversification in R. Meth. Ecol. Evol. 3:1084–1092

Gautier-Hion A., Duplantier J.M., Quris R., Feer F., Sourd C., Decoux J.P., Doubost G., Emmons L., Erard C., Hecketsweiler P., Moungazi A., Roussilhon C., Thiollay J.M. 1985. Fruit characters as a basis of fruit choice and seed dispersal in a tropical forest vertebrate community. Oecologia 65:324–337.

Goldberg E.E., Igic B. 2012. Tempo and mode in plant breeding system evolution. Evolution 66:3701–3709.

Goldberg E.E., Lancaster L.T., Ree R.H. 2011. Phylogenetic inference of reciprocal effects between geographic range evolution and diversification. Syst. Biol. 60:451–465.

Grandcolas P., Murienne J., Robillard T., Desutter-Grandcolas L., Jourdan H., Guilbert E., Deharveng L. 2008. New Caledonia: a very old Darwinian island? Phil. Trans. R. Soc. Lond. B. 363:3309–3317.

Greene D.F., Quesada M. 2005. Seed size, dispersal, and aerodynamic constraints within the Bombacaceae. Am. J. Bot. 92:998–1005.

Guimarães P.R., Galetti M., Jordano P. 2008. Seed dispersal anachronisms: rethinking the fruits extinct megafauna ate. PLoS One 3:e1745.

Hansen J., Sato M., Russell G., Kharecha P. 2013. Climate sensitivity, sea level and atmospheric carbon dioxide. Phil. Trans. R. Soc. A 371:20120294.

Hijmans R.J. 2016. R package 'geosphere'. R package version 1.5-7. Davis, CA: Comprehensive R Archive Network.

Hill R.S. 1995. Chapter 2: conifer origin, evolution, and diversification in the southern hemisphere. In: Enright N.J., Hill R.S., editors. Ecology of the southern conifers. Carlton (VIC): Melbourne University Press. p. 10–29.

Hintze C., Heydel F., Hoppe C., Cunze S., König A., Tackenberg O. 2013. D3: the dispersal and diaspore database—baseline data and statistics on seed dispersal. Persp. Pl. Ecol., Evol. Syst. 15:3180–3192

Hughes L., Dunlop M., French K., Leishman M.R., Rice B. 1994. Predicting dispersal spectra: a minimal set of hypotheses based on plant attributes. J. Ecol. 82:933–950.

Kearse M., Moir R., Wilson A., Stones-Havas S., Cheung M., Sturrock S., Buxton S., Cooper A., Markowitz S., Duran C., Thierer T., Ashton B., Meintjes P., Drummond A. 2012. Geneious basic: an integrated and extendable desktop software platform for the organization and analysis of sequence data. Bioinformatics 28:1647–1649.

Knopf P. 2011. Differentialdiagnose und evolution innerhalb der Podocarpaceae s. l. (Steineibengewächse i. w. S.) [dissertation]. Bochum, Germany: Ruhr-Universität Bochum.

Knopf P., Schulz C., Little D.P., Stützel T., Stevenson D.W. 2012. Relationships within Podocarpaceae based on DNA sequence, anatomical, morphological, and biogeographical data. Cladistics 28(3):27–299.

Landis, M., Matzke, N.J., Moore, B.R., Huelsenbeck, J.P. 2013. Bayesian analysis of biogeography when the number of areas is large. Syst. Biol. 62(6):789–804.

Landis, M.J. 2016. Biogeographic dating of speciation times using paleogeographically informed processes. Syst. Biol. 66:128–144.

Landis, M.J., Freyman, W.A., Baldwin, B.G. 2018. Retracing the Hawaiian silversword radiation despite phylogenetic, biogeographic, and paleogeographic uncertainty. Evolution 72: 2343–2359.

Lanfear, R., Frandsen, P. B., Wright, A. M., Senfeld, T., Calcott, B. 2016. PartitionFinder 2: new methods for selecting partitioned models of evolution for molecular and morphological phylogenetic analyses. Mol. Biol. Evol. 34(3):772–773.

Leprieur F., Descombes P., Gaboriau T., Cowman P.F., Parravicini V., Kulbicki M., Melián C.J., Santana C.N. de, Heine C., Mouillot D., Bellwood D.R., Pellissier L. 2016. Plate tectonics drive tropical reef biodiversity dynamics. Nat. Commun. 7:11461.

Leslie A.B., Beaulieu J.M., Rai H.S., Crane P.R., Donoghue M.J., Mathews S. 2012. Hemisphere-scale differences in conifer evolutionary dynamics. Proc. Nat. Acad. Sci. USA 109:16217–16221.

Lewis P.O. 2001. A likelihood approach to estimating phylogeny from discrete morphological character data. Syst. Biol. 50:913–925.

Little D.P., Knopf P., Schulz C. 2013. DNA barcode identification of Podocarpaceae—the second largest conifer family. PLoS One 8:e81008.

Losos J.B., Ricklefs R.E. 2009. The theory of island biogeography revisited. Princeton (NJ): University Press.

Lowry P.P. 1998. Diversity, endemism, and extinction in the flora of New Caledonia: a review. In: Peng C.I., Lowry P.P., editors. Proceedings of the international symposium on rare, threatened, and endangered floras of Asia and the Pacific. Taipei, Taiwan: Institute of Botany, Academica Sinica. p. 181–206.

Lu, L., Fritsch, P.W., Matzke, N.J., Wang, H., Kron, K.A., Li, D.Z., Wiens, J.J. 2019. Why is fruit colour so variable? Phylogenetic analyses reveal relationships between fruitcolour evolution, biogeography and diversification. Global Ecol. Biogeogr. 1–13.

Maddison W.P., Fitzjohn R.G. 2015. The unsolved challenge to phylogenetic correlation tests for categorical characters. Syst. Biol. 64:127–136.

Magnuson-Ford K., Otto S.P. 2012. Linking the investigations of character evolution and species diversification. Am. Nat. 180:225–245.

Marshall C.R. 2017. Five palaeobiological laws needed to understand the evolution of the living biota. Nat. Ecol. Evol. 1:165.

Matos-Maraví P., Matzke, N.J., Larabee, F.J., Clouse, R.M., Wheeler, W.C., Sorger, D.M., Suarez, A.V., Janda, M. 2019. Taxon cycle predictions supported by modelbased inference in IndoPacific trapjaw ants (Hymenoptera: Formicidae: Odontomachus). Mol. Ecol. 27:4090–4107.

Matzke N.J. 2013. Probabilistic historical biogeography: new models for founder-event speciation, imperfect detection, and fossils allow improved accuracy and model-testing. Front. Biogeogr. 5:242–248.

Matzke, N.J. 2014. Model selection in historical biogeography reveals that founder-event speciation is a crucial process in island clades. Syst. Biol. 63(6):951–970.

Matzke N.J., Wright A. 2016. Inferring node dates from tip dates in fossil Canidae: the importance of tree priors. Biol. Lett. 12: 20160328.

McDonald-Spicer, C., Knerr, N.J., Encinas-Viso, F., Schmidt-Lebuhn, A.N. 2019. Big data for a large clade: Bioregionalization and ancestral range estimation in the daisy family (Asteraceae). J. Biogeogr. 46:255–267.

Meyer-Berthaud B., Taylor T.N. 1991. A probable conifer with podocarpaceous affinities from the Triassic of Antarctica. Rev. Palaeobot. Palyn. 67:179–198.

Mortimer N., Campbell H.J., Tulloch A.J., King P.R., Stagpoole V.M., Wood R.A., Rattenbury M.S., Sutherland R., Adams C.J., Collot J., Seton M. 2017. Zealandia: Earth's Hidden Continent. GSA Today 27:27–35.

Müller R.D., Qin X., Sandwell D.T., Dutkiewicz A., Williams S.E., Flament N., Maus S., Seton M. 2016. The GPlates Portal: cloud-based Interactive 3D visualization of global geophysical and geological data in a web browser. PLoS One 11:e0150883.

Murienne J., Grandcolas P., Piulachs M.D, Bellés X., D'Haese C., Legendre F., Pellens R., Guilbert E. 2005. Evolution on a shaky piece of Gondwana: is local endemism recent in New Caledonia? Cladistics 21:2–7.

Nash J.C., Varadhan R. 2011. Unifying optimization algorithms to aid software system users: optimx for R. J. Stat. Softw. 43:1–14.

Nathan R. 2006. Long-distance dispersal of plants. Science 313: 786–788.

Paradis E., Claude J., Strimmer K. 2004. APE: analyses of phylogenetics and evolution in R language. Bioinformatics 20:289–290.

Prum R.O., Berv J.S., Dornburg A., Field D.J., Townsend J.P., Lemmon E.M., Lemmon A.R. 2015. A comprehensive phylogeny of birds (Aves) using targeted next-generation DNA sequencing. Nature 526:569–573.

Pyron R.A. 2017. Novel approaches for phylogenetic inference from morphological data and total-evidence dating in squamate reptiles (lizards, snakes, and amphisbaenas). Syst. Biol. 66:38–56.

Quiroga M.P., Mathiasen P., Iglesias A., Mill R.R., Premoli A.C., 2016. Molecular and fossil evidence disentangle the biogeographical history of Podocarpus, a key genus in plant geography. J. Biogeogr. 43:372–383.

Rea D.K., Zachos J.C., Owen R.M., Gingerich P.D. 1990. Global change at the Paleocene-Eocene boundary: climatic and evolutionary consequences of tectonic events. Palaeogeogr. Palaeoclim. Palaeoecol. 79:117–128.

Ree, R.H., Sanmartín, I. 2018. Conceptual and statistical problems with the DEC+J model of founderevent speciation and its comparison with DEC via model selection. J. Biogeogr. 45(4):741–774.

Ree R.H., Smith S.A. 2008. Maximum likelihood inference of geographic range evolution by dispersal, local extinction, and cladogenesis. Syst. Biol. 57:4–14.

Schulz C., Klaus K.V., Knopf P., Mundry M., Dörken V., Stützel T. 2014. Male cone evolution in conifers: not all that simple. Am. J. Plant Sci. 5:2842–2857.

Sorensen A.E. 1986. Seed dispersal by adhesion. Ann. Rev. Ecol. Syst. 17:443–463.

Sukumaran J., Economo E.P., Knowles L.L. 2016. Machine learning biogeographic processes from biotic patterns: a new trait-dependent dispersal and diversification model with model choice by simulation-trained discriminant analysis. Syst. Biol. 65:525–545.

Sukumaran, J., Knowles, L.L., 2018. Trait-dependent biogeography: (re) integrating biology into probabilistic historical biogeographical models. Trends Ecol. Evol. 33(6):390–398.

Swenson U., Nylinder S., Munzinger J. 2014. Sapotaceae biogeography supports New Caledonia being an old Darwinian island. J. Biogeogr. 41:797–809.

Uyeda J.C., Zenil-Ferguson R., Pennell M.W. 2018. Rethinking phylogenetic comparative methods. Syst. Biol. 67:1091–1109.

Vaidya G., Lohman D.J., Meier R. 2011. SequenceMatrix: concatenation software for the fast assembly of multi-gene datasets with character set and codon information. Cladistics 27:171–180.

Van Dam M.H., Matzke N.J. 2016. Evaluating the influence of connectivity and distance on biogeographical patterns in the south-western deserts of North America. J. Biogeogr. 43:1514–1532.

Van Den Elzen, C.L., LaRue E.A., Emery N.C. 2016. Oh, the places you'll go! Understanding the evolutionary interplay between dispersal and habitat adaptation as a driver of plant distributions. Am. J. Bot. 103:2015–2018.

Viseshakul N., Charoennitikul W., Kitamura S., Kemp A., Thong-Aree S., Surapunpitak Y., Poonswad P., Ponglikitmongkol M. 2011. A phylogeny of frugivorous hornbills linked to the evolution of Indian plants within Asian rainforests. J. Evol. Biol. 24:1533–1545.

Vittoz P., Engler R. 2007. Seed dispersal distances: a typology based on dispersal modes and plant traits. Bot. Helv. 117:109.

Wagstaff S.J. 2004. Evolution and biogeography of the austral genus *Phyllocladus* (Podocarpaceae). J. Biogeogr. 31:1569–1577.

Webb, C.O. Ree, R.H. 2012. Historical biogeography inference in Malesia. In: Gower D., Johnson K., Richardson J., editors. Biotic evolution and environmental change in Southeast Asia. Cambridge: Cambridge University Press. p. 191–215.

Weir J.E., Corlett R. 2007. How far do birds disperse seeds in the degraded tropical landscape of Hong Kong, China? Landscape Ecol. 22:131–140.

Wickham, H. 2011. testthat: get started with testing. R J 3(1):5–10.

Willson M.F., Graff D.A., Whelan C.J. 1990. Color preferences of frugivorous birds in relation to the colors of fleshy fruits. Condor 92:545–555.

Xiang Y., Gubian S., Suomela B., Hoeng J. 2013. Generalized simulated annealing for global optimization: the GenSA package. R J 5:13–29.

Zachos J.C., Dickens G.R., Zeebe R.E. 2008. An early Cenozoic perspective on greenhouse warming and carbon-cycle dynamics. Nature 451:279–283.